sustainability

MDPI

Article

Study on the permeability improved technology of fracturing coal seam based on liquid carbon dioxide

Feng Zhang [1,2,3]*, Jinshan Zhang [1], Xuping Li[1], Dongjuan Dong[1]

[1] School of Mine and Coal, Inner Mongolia University of Science and Technology, Baotou 014010, Inner Mongolia, China
[2] State Key Laboratory of Gas Disaster Monitoring and Emergency Technology, Chongqing 400037, China
[3] China Coal Technology and Engineering Group Chongqing Research Institute, Chongqing 400037, China

Abstract: For the problem of low drainage rate in the low permeability coal seam, this paper studied the technology of permeability improved by carbon dioxide. The COMSOL was used to determine the influence radius of liquid carbon dioxide phase transition cracking was 13.4 m, and designed the scheme of boreholes. The field test was carried out in the 81506 working face of Baode Coal Mine. Through the on-site monitoring data of the extraction volume of the 100-meter borehole, the gas concentration of the borehole, and the gas permeability coefficient of the coal seam, the results showed that the drainage effect was increased by 293.9%, the gas drainage concentration was increased by 242.4%, the permeability coefficient of the coal seam was increased by 3–7.75 times, and the permeability enhancement effect was good.

Keywords: coal seam permeability, gas drainage, coal seam permeability improvement, carbon dioxide fracturing

Citation: Lastname, F.; Lastname, F.; Lastname, F. Title. *Sustainability* **2022**, *14*, x. https://doi.org/10.3390/xxxxx

Academic Editor: Firstname Lastname

Received: date
Accepted: date
Published: date

1. Introduction

For a long time, gas has seriously restricted the safety production of coal mine enterprises [1–3]. In recent years, with the increase of mining depth, the permeability of coal seam has become lower and lower. How to enhance the permeability of coal seam is a prerequisite for gas extraction and safe production of coal mines. At present, hydraulic fracturing technology is widely used in gas extraction, especially for the upward layer-through borehole, the effect of hydraulic fracturing is better [4–6]. However, the effect of coal seam permeability improvement is poor for the downward layer-through borehole. The influence of different thickness and hardness of coal seam on the effect of permeability enhancement is less studied, and the understanding of the coal breaking mechanism of hydraulic punching, the mechanism of increasing permeability and pressure relief is not enough, and the process and technical parameters of hydraulic punching need to be further studied. The commonly punching process is easy to cause problems such as holding holes, plugging holes, sticking, and running water. In particular, the coal-water mixture flushed from the upward hole tends to accumulate at the upper opening of the casing, which directly affects the drilling and flushing process [7–9]. Therefore, there is an urgent need to find a penetration enhancement method with good penetration effect and high safety, which can be widely used. This paper analyzes and researches the anti-permeability technology of liquid CO_2 fracturing coal seam.

2. Study on the permeability improved technology of liquid carbon dioxide

The liquid carbon dioxide phase transition cracking device uses a heating tube to heat the liquid carbon dioxide in the liquid storage tube, making it change from a liquid state to a gas state, and the pressure increases sharply [10–12]. Then the high-pressure gas smashes the constant pressure energy release sheet, and generates stress waves that propagate around. The generated gas passes through the release channel of the exhaust pipe and reaches the surface of the coal mass in a short time to form an explosive airflow. Stress waves and high-energy gas can not only generate new cracks in the coal mass, but also make the original cracks expand and develop to fracture the coal seam [13–15].

2.1. Effect of stress wave on coal mass

When high-pressure carbon dioxide gas is ejected from the liquid storage pipe, it is accompanied by the generation of stress waves. When the coal mass is regarded as an ideal elastomer, the motion equation of the coal-rock particle when the elastic wave propagates is as follows:

$$(\lambda + G)\frac{\partial \theta}{\partial x_i} + G\nabla^2 u_i = \rho \frac{\partial^2 u_i}{\partial t^2} \quad i=1,2,3\ldots \tag{1}$$

where u_i is the displacement of the particle in the coordinate direction; $\theta = \varepsilon_{ij} = u_{ij}$, volumetric strain; ∇^2 is the laplace operator; λ, G is the lame elastic constant; ρ is the density of coal-rock mass; t is time.

2.2. High pressure gas gathering cutting by phase change of liquid carbon dioxide

The special design of the end of the release pipe in the liquid carbon dioxide phase transition equipment can solve the problem of blasting energy dispersion and dilution. The exhaust hole of the release pipe allows the gas to be discharged in a fixed direction, so that the energy is gathered and fractures the coal mass. When the high-pressure liquid carbon dioxide gas impacts the coal in the form of jet, the high-pressure gas will radiate from the center of the jet, as shown in Figure 1.

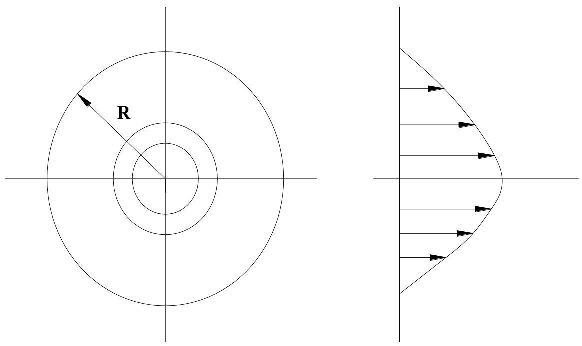

Figure 1. Pressure distribution of pressurized gas jet on the vertical impact of medium.

The impact of high-pressure carbon dioxide gas to fracture the coal mass is divided into the following categories: cavitation damage; impact cutting effect of high-pressure gas; dynamic pressure effect of high-pressure gas; gas wedge effect formed by high pressure gas. Under the impact of high-pressure carbon dioxide gas, the internal stress distribution of the coal mass is similar to the half-space elastomer under the concentrated load. When the compressive stress generated by the impact of high-pressure gas reaches or exceeds the compressive strength of the coal body, the original coal body is damaged, and cracks are formed in the coal body. When the compressive stress generated by the impact of high-pressure gas exceeds the compressive strength of the coal mass, the original coal mass is damaged, and cracks are formed. As shown in Figure 2, the high-pressure gas entering into the cracks makes the cracks develop and expand rapidly, resulting in the fracture of the coal seam.

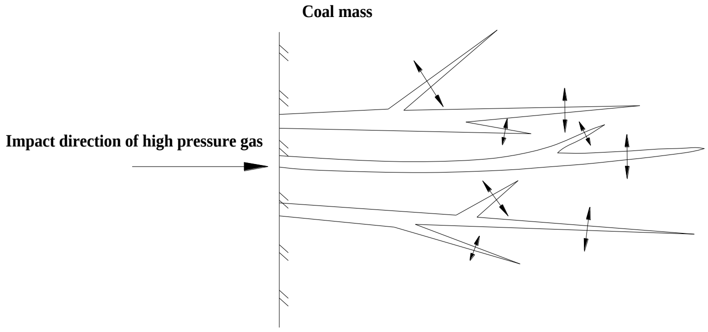

Figure 2. High-pressure carbon dioxide gas cutting the coal seam.

2.3. Coal seams fractured by liquid carbon dioxide phase change expansion force

The liquid carbon dioxide in the liquid storage pipe gradually changes into gaseous carbon dioxide after heating, the volume expands continuously, and the pressure of the carbon dioxide gas increases continuously [16–18]. When the carbon dioxide gas breaks through the constant pressure valve and is ejected through the release pipe, the carbon dioxide gas still expands and increases, generating expansion work [19–21]. On the one hand, the high-pressure carbon dioxide gas exerts pressure on the wall of the fracturing boreholes, forcing new fractures in the coal seam; on the other hand, the high-pressure carbon dioxide gas enters the coal seam and expands the original fractures in the coal seam.

3. Numerical simulation of influence radius

3.1. Numerical model

In order to study the influence radius of liquid carbon dioxide phase transition cracking, taking the #8 coal seam of Baode Coal Mine China as the engineering background, the COMSOL was used for analysis. For the convenience of simulation, the phase transition process of liquid carbon dioxide was simplified. In the numerical calculation, a gas pressure of 270 MPa was applied to simulate the cracking gas pressure generated during the phase transition of liquid carbon dioxide. The parameters of coal mass were shown in Table 1.

Table 1. The parameters of the model.

Symbol	Parameter	Value	Unit
ρ_1	Density of coal seam	1490	kg/m^3
E	Elastic modulus	2×10^9	Pa
V	Poisson ratio	0.35	–
K	Permeability	10^{-17}	m^2
K_1	Porosity	6.58	%
c	Cohesion	4	MPa
φ	Internal friction angle	33	°
ρ_2	Density of CO_2	1.977	kg/m^3
μ	Dynamic viscosity of CO_2	1.48×10^{-5}	Pa•s
Z	Compressibility factor of CO_2	1.02	–

The model was constructed with the 81506 working face of Baode Coal Mine as the engineering background, and the model was shown in Figure 3. The size of the model was 150m×100m, and the fracturing boreholes was located in the middle of the calculation model. To facilitate the calculation, the mesh size was differentiated. The mesh size near the fracturing boreholes was small and dense, and the mesh size away from the fracturing boreholes was large and sparse [22–24]. The boundary of the model was fixed, the diameter of the borehole was 113 mm. The boundary condition of the orifice was Darcy's law, and the pressure was 270 MPa. The upper boundary of the model was subject to uniformly distributed original rock stress.

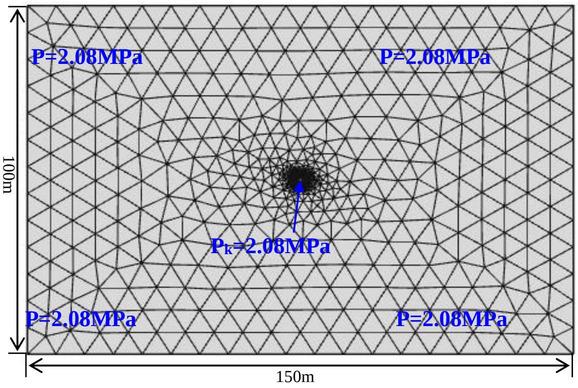

Figure 3. Numerical model.

3.2. Features of plastic deformation

According to the numerical model and the stress applied to the model, the plastic deformation characteristics of the coal mass around the borehole after phase transition cracking were simulated, which was shown in Figure 4(a). To analyze the damage area of high pressure gas on the coal mass, a section was made in the middle of the coal mass, which was shown in Figure 4(b).

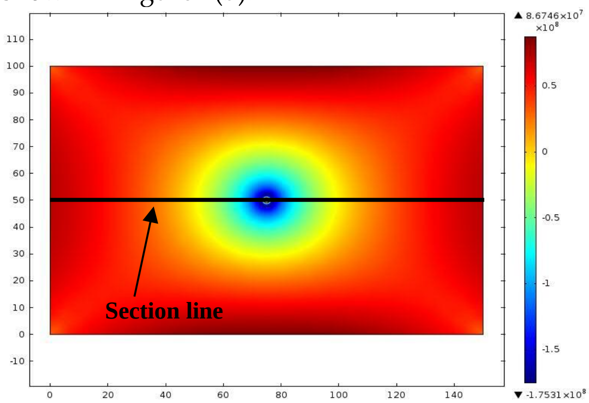

(a) Plastic deformation area

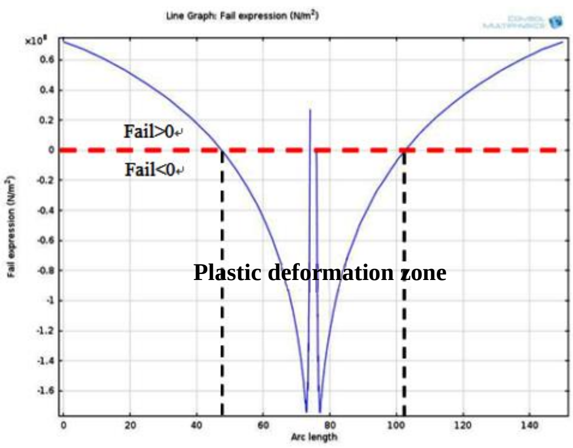

(b) Sectional view of plastic deformation area

Figure 4. Plastic deformation.

Increasing the pore pressure was equivalent to applying a tensile stress to the coal matrix. Due to the tensile stress, cracks in the coal matrix begin to develop and expand, and finally plastic deformation occurs in the coal matrix. Under the condition that the gas pressure of 270 MPa was applied at the orifice, Fail = 0 meant it was in a critical state of destruction; Fail < 0 meant that plastic deformation had occurred; Fail > 0 meant it was in a stable state. The numerical simulation results showed that the radius of plastic deformation of the coal matrix was 23 m. According to the numerical simulation, the plastic deformation region of the coal matrix was divided as follows, the area of Fail < 1.0×-10^8 Pa was the broken circle, the radius r_1 was about 4.6 m; the area of 1.0×-10^8 Pa < Fail < 0.5×-10^8 Pa was the fissured circle, the radius was 4.6 m< r_2 <13.4 m; the area of 0.5×-10^8 Pa < Fail < 0 was the disturbance circle, the radius was 13.4 m< r_3< 23.1 m. The area was divided as shown in Figure 5.

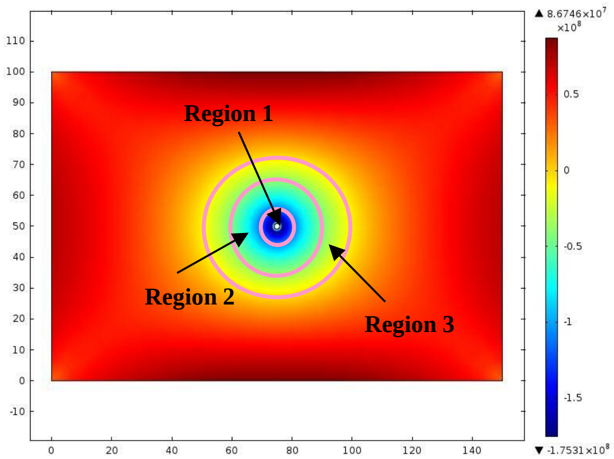

Figure 5. Division of the plastic deformation zone.

As shown in Figure 5, the plastic damage of the broken circle was the most serious, the plastic damage of the fracture circle was smaller, and the plastic damage of the disturbance circle was the smallest, but it still had a promotion effect on gas drainage. To make the borehole had good gas drainage effect, the borehole should be arranged within the range of the fissured circle. According to the numerical simulation, the influence radius of the fissured circle was 13.4 m.

3.3. Features of the volumetric strain

In order to improve the accuracy of the division of different regions, the volumetric strain obtained during the simulation process by COMSOL, as shown in Figure 6(a). According to the position of the section line in Figure 5, the volumetric strain contour in Figure 6(a) is cross-sectioned, and the result is shown in Fig. 6(b).

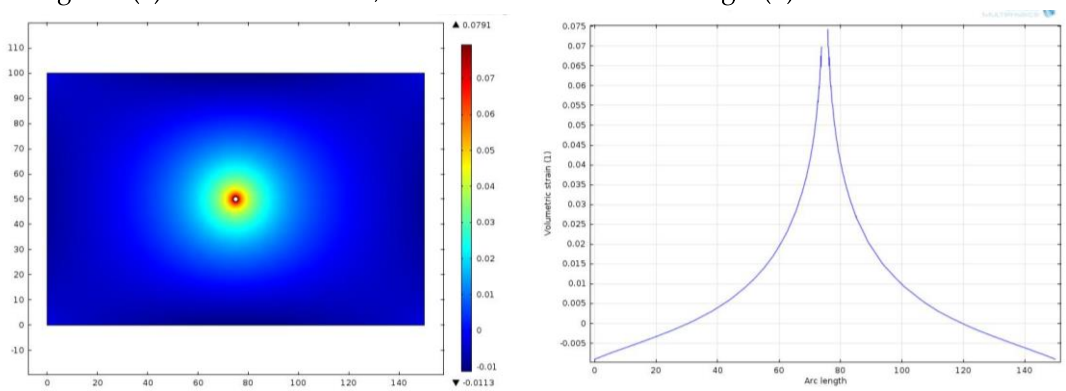

(a) The nephogram of volumetric strain **(b) The section value of volumetric strain**

Figure 6. The volumetric strain.

As shown in Figure 6, when a gas pressure of 270 MPa was applied at the orifice, the volumetric strain of the coal matrix showed that the closer the distance to the orifice, the larger of the volumetric strain. The distribution of volumetric strain was consistent with the distribution of plastic deformation of coal matrix. The volumetric strain in the broken circle was the largest, followed by the fissured circle, and the disturbance circle was the smallest.

4. Field test

4.1. Engineering Background

According to the current situation of the Baode Coal Mine, the 81506 working face in the five-panel area was selected as the field test site for liquid carbon dioxide fracturing and permeability enhancement. The 81506 working face had a buried depth of 375 m~450 m, the original gas content was 4.6 m^3/t~6.8 m^3/t, the average gas content was 5.7 m^3/t, and the maximum gas pressure was 1.7 MPa. The structure of the coal seam was complex, with 3–4 layers of gangue, and the average coal thickness was 8.4m. The roof and floor strata of the coal seam were shown in Table 2.

Table 2. The roof and floor strata of the coal seam.

Strata	Lithology	Thickness/m
Main roof	Medium sandstone, Mudstone	10
Immediate roof	Siltstone, Sandy mudstone	8.4
Immediate floor	Siltstone	5.6
Main floor	Grit stone	5.3

4.2. Test scheme

According to the numerical simulation, combined with the field construction experience, the fracturing test was carried out in the 81506 working face. As shown in Figure 7, two types of drilling holes, fracturing boreholes and contrast boreholes, were arranged in the 81506 working face. The fracturing boreholes were arranged at intervals of 20m in the reserved area of the 81506 working face. The borehole depths were 220m, 140m, 144m, 142m, 125m, and 125m. respectively, and the borehole diameter was 113mm. The contrast boreholes were arranged in the 100m area on both sides of the fracturing area.

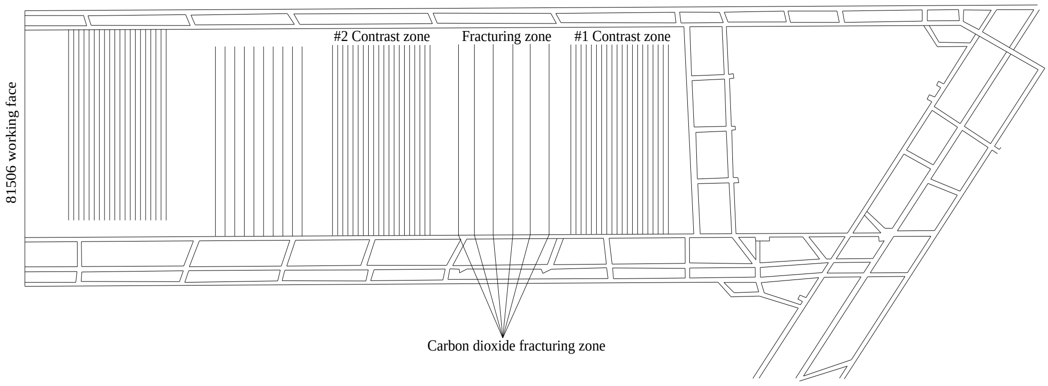

Figure 7. The arrangement of boreholes.

4.3. The effect of fracturing

(1) Gas extraction volume and gas extraction concentration

The on-site monitoring curves of the gas extraction volume of the fracturing boreholes and contrast boreholes were shown in Figure 8.

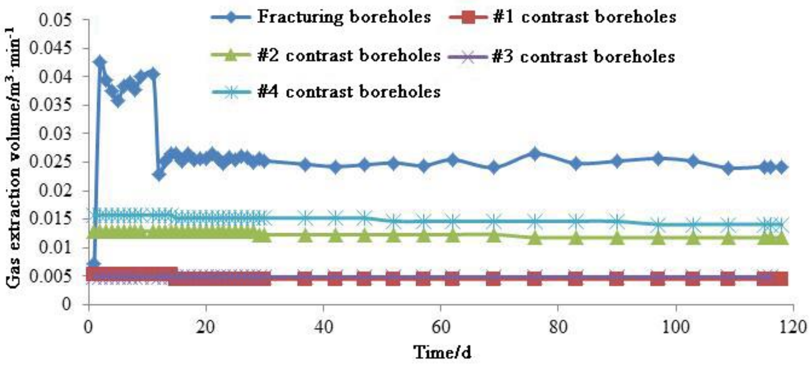

Figure 8. The arrangement of boreholes.

As shown in Figure 8, the gas drainage volume of the fracturing boreholes was significantly higher than that of the contrast boreholes during the same period. According to the on-site monitoring data, the maximum and average values of gas drainage in the fracturing boreholes and contrast boreholes were shown in Table 3.

Table 3. Gas drainage volume of fracturing boreholes and contrast boreholes.

Type	Gas drainage volume	
	Maximum value	Mean value
Fracturing boreholes	0.0426	0.0276
#1 contrast boreholes	0.0052	0.0046
#2 contrast boreholes	0.0129	0.0122
#3 contrast boreholes	0.0049	0.0049
#4 contrast boreholes	0.0158	0.0148

As shown in Table 3, the gas extraction volume of the fracturing boreholes was 186-600% of the gas extraction volume of the contrast boreholes, with an average of 393.9%, and the extraction effect of the fracturing boreholes was 293.9% higher than that of the contrast boreholes on average. The monitoring curves of gas drainage concentration in fracturing boreholes and contrast boreholes were shown in Figure 9.

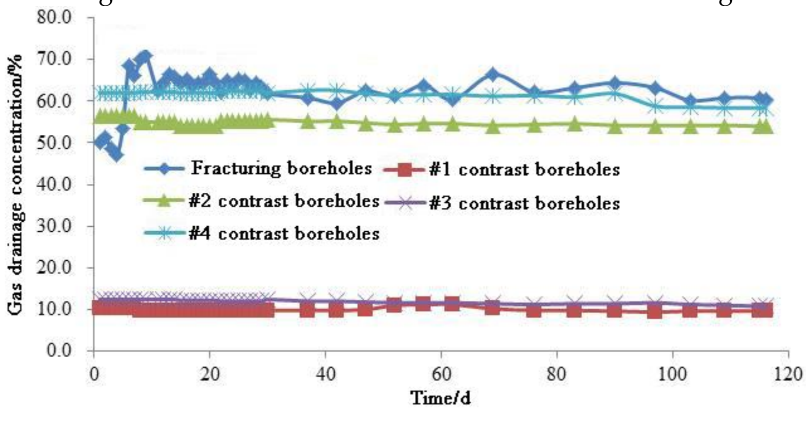

Figure 9. Monitoring curves of gas drainage concentration.

As shown in Figure 9, the gas drainage concentration of the fracturing boreholes was close to that of the contrast boreholes with higher gas drainage concentration, but was significantly higher than that of the contrast boreholes with lower gas concentration. According to the on-site monitoring data, the maximum and average values of gas drainage in the fracturing boreholes and contrast boreholes were shown in Table 4.

Table 4. Gas drainage concentration of fracturing boreholes and contrast boreholes.

Type	Gas drainage concentration/%	
	Maximum value	Mean value
Fracturing boreholes	71	62.3
#1 contrast boreholes	11.2	9.9
#2 contrast boreholes	56.4	55
#3 contrast boreholes	12.4	12
#4 contrast boreholes	62.6	61.6

As shown in Table 4, the maximum gas extraction concentration of the fracturing boreholes was 113.4~633.9% of the gas extraction concentration of the contrast boreholes, and the average value was 101.6~632.3%. The maximum and average of the gas extraction concentration of the fracturing boreholes were higher than those of the contrast boreholes, and the concentration of gas drainage increased by 242.4% on average.

(2) Coal seam permeability coefficient

The coal seam gas content was measured before and after fracturing, and the natural gas flow rate of the borehole was measured. The coal seam permeability coefficient before and after fracturing the coal seam in the #3 and #5 panels were shown in Table 5.

Table 5. The coal seam permeability coefficient.

Location	The coal seam permeability coefficient $m^2/MPa^2 \cdot d$		Multiple
	Before fracturing	After fracturing	
#3 panel	0.052755	0.159058	3.01
#5 panel	0.030846	0.23915	7.75

As shown in Table 5, the permeability coefficient of coal seam increases by 3–7.75 times after fracturing, and the effect of increasing the permeability coefficient of coal seam by liquid carbon dioxide fracturing was obvious.

4.4. Analysis of test results

According to the field test data, the conclusions were as follows,

(1) In the first month after carbon dioxide fracturing in the 81506 working face of the #5 panel, the gas extraction volume increased by 306% compared with the contrast boreholes; four months after fracturing, the gas drainage volume of the fracturing boreholes increased by 293.9% compared with the contrast boreholes.

(2) The maximum and average values of the gas extraction concentration in the fracturing boreholes were both greater than those in the contrast boreholes. The average gas concentration of the fracturing boreholes was 1.76 times that of the contrast boreholes, an average increase of 242.4%.

(3) After fracturing, the permeability coefficient of coal seam increased by 3–7.75 times, and the effect of increasing the permeability coefficient of coal seam by carbon dioxide fracturing was obvious.

5. Conclusion

In this paper, the mechanism of the liquid carbon dioxide coal seam anti-permeability technology was preliminarily studied, and the Comsol software was used to numerically analyze the influence radius of liquid carbon dioxide phase transition fracturing, which provides a basis for reasonable field distribution parameters, and analyze the effect of on-site liquid carbon dioxide fracturing, the main conclusions were as follows,

(1) The technology of liquid carbon dioxide fracturing to improve coal seam permeability through three aspects. First, the action of stress wave causes new cracks to form in the coal mass, and stress concentration occurs at the tip of the crack, which promotes the expansion and development of tiny cracks. Second, the intrusion of high-pressure liquid

carbon dioxide gas into the coal, resulting in cutting, impact, gas wedge and other effects. Third, the carbon dioxide gas breaks through the constant pressure valve, a large expansion thrust is generated, which acts on the coal mass, generating new cracks and disturbing the primary cracks in the coal seam.

(2) The COMSOL software was used to simulate the influence radius of liquid carbon dioxide cracking, and it was determined that under the geological conditions of the 8# coal seam in Baode Coal Mine, the influence radius of carbon dioxide phase transition cracking was 13.4 m.

(3) The gas extraction volume, gas concentration, and coal seam permeability coefficient of the fracturing hole and the contrast hole were monitored on site. The results showed that the fracturing effect was good.

Author Contributions: Conceptualization, F.Z.; methodology, F.Z.; software, J.Z.; validation, X.Li.; formal analysis, F.Z.; investigation, J.Z.; resources, J.Z.; data curation, F.Z.; writing—original draft preparation, F.Z.; writing—review and editing, H.D.; visualization, H.D.; supervision, X.L.; project administration, J.Z.; funding acquisition, F.Z. All authors have read and agreed to the published version of the manuscript."

Funding: This research is financially supported by the Higher educational scientific research projects of Inner Mongolia Autonomous Region (No. NJZY21291).

Institutional Review Board Statement: "Not applicable" for studies not involving humans or animals.

Informed Consent Statement: "Not applicable" for studies not involving humans.

Data Availability Statement: All data included in this study are available upon request by contacting the corresponding author.

Acknowledgments: We are grateful to anonymous reviewers for their constructive reviews on the manuscript, and the editors for carefully revising the manuscript.

Conflicts of Interest: The authors declare no conflicts of interest.

References

1. Kang XB, Luo S, Li QS et al (2017) Developing a risk assessment system for gas tunnel disasters in China. J MT SCI-ENGL 14(9):1751-1762
2. Wang K, Du F (2020) Coal-gas compound dynamic disasters in China: A review. PROCESS SAF ENVIRON 133:1-17
3. Chen XJ, Li LY, Wang L et al (2019) The current situation and prevention and control countermeasures for typical dynamic disasters in kilometer-deep mines in China. SAFETY SCI 155:229-236
4. Hu GZ, Sun C, Sun MF et al (2018) The case for enhanced coalbed methane using hydraulic fracturing in the geostructural belt. ENERG EXPLOR EXPLOIT 36(6):1629-1644
5. Lu WY, He CC (2020) Numerical simulation of the fracture propagation of linear collaborative directional hydraulic fracturing controlled by pre-slotted guide and fracturing boreholes. ENG FRACT MECH 235. https://doi.org/10.1016/j.engfracmech.2020.107128
6. Yang W, Lu CZ, Si GY et al (2020) Coal and gas outburst control using uniform hydraulic fracturing by destress blasting and water-driven gas release. J NAT GAS SCI ENG 79. https://doi.org/10.1016/j.jngse.2020.103360
7. Wang YL, Yu ZJ, Wang ZF (2018) A Mechanical Model of Gas Drainage Borehole Clogging under Confining Pressure and Its Application. ENERGIES 11(10). https://doi.org/10.3390/en11102817
8. Sun XY, Cheng ZH, Chen L et al (2021) Deflection laws of gas drainage boreholes in interbedded soft and hard seams: a case study at Xinzheng Coal Mine, China. ADV CIV ENG 2021. https://doi.org/10.1155/2021/5533879
9. Hu CW, Li Q, Wang YL et al (2022) Influence mechanism of mine pressure on coal seam gas emission during mining. Geotech Geol Eng 2022. https://doi.org/10.1007/s10706-022-02078-w
10. Zhang YA, Deng JR, Deng HW et al (2019) Peridynamics simulation of rock fracturing under liquid carbon dioxide blasting. INT J DAMAGE MECH 28(7):1038-1052
11. Xia JQ, Dou B, Tian H et al (2021) Research on initiation of carbon dioxide fracturing pipe using the liquid carbon dioxide phase-transition blasting technology. ENERGIES 14(3). https://doi.org/10.3390/en14030521
12. Chen HD, Wang ZF, Qi LL (2017) Effect of liquid carbon dioxide phase change fracturing technology on gas drainage. ARAB J GEOSCI 10(14). https://doi.org/10.1007/s12517-017-3103-0
13. Zhang YA, Deng JR, Ke B (2018) Experimental study on explosion pressure and rock breaking characteristics under liquid carbon dioxide blasting. ADV CIV ENG 2018. https://doi.org/10.1155/2018/7840125
14. Ishida T, Aoyagi K, Niwa T (2012) Acoustic emission monitoring of hydraulic fracturing laboratory experiment with supercritical and liquid CO2. GEOPHYS RES LETT 39. https://doi.org/10.1029/2012GL052788

15. Niezgoda T, Miedzinska D, Malek E (2013) Study on carbon dioxide thermodynamic behavior for the purpose of shale rock fracturing. B POL ACAD SCI-TECH 61(3):605-612
16. Li Q, Wang YL, Owusu AB (2019) A modified Ester-branched thickener for rheology and wettability during CO2 fracturing for improved fracturing property. ENVIRON SCI POLLUT R 26(20):20787-20797
17. Liao ZW, Liu XF, Song DZ et al (2020) Micro-structural damage to coal induced by liquid CO2 phase change fracturing. NAT RESOUR RES 30(2):1613-1627
18. Liu H, Wang F, Zhang J et al (2014) Fracturing with carbon dioxide: Application status and development trend. PETROL EXPLOR DEV+ 41(4):513-519
19. Rogala A, Ksiezniak K, Krzysiek J et al (2014) Carbon dioxide sequestration during shale gas recovery. PHYSICOCHEM PROBL MI 50(2):681-692
20. Yang ZZ, Yi LP, Li XG et al (2018) Phase control of downhole fluid during supercritical carbon dioxide fracturing. GREENH GASES 8(6):1079-1089
21. Hu CW, Yang XJ, Huang RF et al (2020) Presplitting blasting the roof strata to control large deformation in the deep mine roadway. ADV CIV ENG 2020. https://doi.org/10.1155/2020/8886991
22. Yang XJ, Hu CW, Liang JH et al (2019) A case study on the control of large deformations in a roadway located in the Du'erping coal mine in China. ADV MATER SCI ENG 2019. https://doi.org/10.1155/2019/9628142
23. Jovanovic AP, Stankov MN, Loffhagen D et al (2021) Automated fluid model generation and numerical analysis of dielectric barrier discharges using Comsol. IEEE T PLASMA SCI 49(11):3710-3718
24. Hu CW, Liu W, Wang YT (2020) Study on the influence of the location of dirt band on top coal caving property in extra-thick coal seam. Geotech Geol Eng 38(6). https://doi.org/10.1007/s10706-020-01430-2